

# SEISMOCARDIOGRAM RECORDS PRESSURE OF THE HEART VENTRICLES ON THE RIBS

Viatcheslav Gurev<sup>1</sup>, Kouhyar Tavakolian<sup>2</sup>, Jason Constantino<sup>1</sup>, Bozena Kaminska<sup>2</sup>,  
Natalia A. Trayanova<sup>1</sup>

*Department of Biomedical Engineering and Institute for Computational Medicine, Johns  
Hopkins University, Baltimore, MD, USA<sup>1</sup>*

*The School of Engineering Science, Simon Fraser University, British Columbia, Canada<sup>2</sup>*

## INTRODUCTION

Diagnostic tools to identify cardiac pathologies are based on measurements of the electrical (electrocardiography, noninvasive electrocardiographic imaging) and mechanical (ultrasound and magnetic resonance imaging (MRI)) activity of the heart. However, unlike electrocardiography, imaging of mechanical deformations in the ventricular walls requires relatively expensive clinical equipment. This problem can be partially solved by using seismocardiography, the mechanical analog of electrocardiography.

Sternum seismocardiogram (SCG) is a recording of the heart beating using the signal generated from an accelerometer placed on the sternum. It has been shown that several peaks of the seismocardiogram coincide with specific events of the cardiac cycle, such as the opening and closing of the heart valves [1-3]. The amplitude and morphology of the signal change depending on different factors that include respiration [4], cardiac contractility [5], and heart rhythm [6]. Although sternum seismocardiography was first employed over two decades ago, its clinical application and advancement are still limited, owing to the fact that the mechanisms underlying the morphology of the signal remain unclear. In the previous study from our group, SCG was simulated using an anatomically-accurate 3D electromechanical model of the heart ventricles [7]. Although the computational model reliably reproduced the clinically-observed peaks in the SCG during isovolumic contraction and ventricular filling phases, it failed to capture other peaks during ejection and relaxation phases. Moreover, the model was unable to reproduce changes in morphology of the signal during respiration cycles that are observed clinically.

In this paper, we improve our 3D model of ventricular contraction by including representation of the pressure acting on the ventricles by the chest. As compared to our previous study, this new model captures major cardiac events including ejection phase of the cardiac cycle. In addition, the model also provides mechanistic insight to the changes in SCG signal morphology during inspiration and expiration.

## METHODS

### Electromechanical model

The image-based 3D electromechanical model of the canine ventricles (Figure 1A) has been described in our previous study [7]. Details related to multiscale modeling of ventricular contraction can be found in a review publication [8]. Briefly, the geometry of the model is based on MRI with fiber and laminar sheet geometry determined from diffusion tensor MRI. Electromechanical activity of the heart is simulated by using the monodomain model of electrical propagation, an ionic model of membrane kinetics, a biophysical model of the cardiac myofilaments, and a continuous model of passive cardiac mechanics. The ventricular model is coupled with a circulatory model to simulate the different phases of the cardiac cycle. Lastly, the surrounding anatomical structures such as the ribs and internal organs are incorporated (see below).

### Representation of the sternum and internal organs

The ribs were represented as a solid cylinder of 10mm radius that was placed next to the right ventricular apex (Figure 1B), in accordance with the thoracic position of the heart observed from publicly available cine-MRI videos [9]. Since the displacement of the ribs due to contraction of the ventricles is much smaller than the movement of the ventricular walls and does not affect cardiac mechanics, the position of the cylinder was static and changed only during respiration phases. Pressure of the cylinder on the ventricular surface  $P_c$  (as well as pressure of the ventricles on the cylinder) was simulated using a penalty term, which increased exponentially with the difference between the distance  $d$  of the point on the ventricular surface from the axis of the cylinder, and the radius of the cylinder  $r$ :

$$P_c = \begin{cases} \alpha(e^{\beta \times (r-d)} - 1), & d < r \\ 0, & \text{otherwise} \end{cases}, \quad (1)$$

where  $\alpha=1\text{kPa}$  and  $\beta=5\text{mm}^{-1}$ . Internal thoracic organs that surround the heart were simulated as a cylinder of

radius 100mm that was placed behind the posteriolateral wall of the left ventricle (LV).

Since the orientation of the ribs changes during inspiration and expiration, simulations were performed with a control orientation of the ribs (Figure 1B) and a rotated orientation, where the ribs were oriented 15 degrees more in the longitudinal direction of the ventricles than in the control case.

### SCG signal

SCG signal was represented as a function of pressure on the rib cylinder. Since mechanical properties of the sternum during contraction are unknown, two limiting cases were considered: when the elastic term is much greater than the viscous term (elastic case) and when the viscous term is significantly larger than the elastic term (viscous case) of the Kelvin–Voigt model. Thus, the acceleration of the chest was proportional to either the first or second temporal derivative of the pressure on the rib cylinder for the viscous or elastic case, respectively.

The experimental SCG signals were recorded by placing piezoelectric accelerometer on the sternum in the midline with its lower edge at the xiphoid process. The sensor is model 393C from PCB Piezotronics that has a linear response between 0.3 and 800Hz and sensitivity of 1.0 V/g.

## **RESULTS**

### Morphology of the simulated SCG signal

Normalized SCG signals for cases when the rib was considered an elastic (top) and viscous (middle) material and the temporal changes in LV volume (bottom) are shown in Figure 1C. Clinically recorded SCG phases are shown in Figure 1D for comparison. Although the SCGs in the elastic and viscous cases look similar, only the viscous case reproduces key features of the SCG signal. Consistent with previous publications [1-3], the global positive peak occurs at the instant of aortic valve opening (the beginning of the ejection phase during which the LV volume decreases). During ejection, there is a rapid decrease followed by a slow increase in acceleration (2). Lastly, local negative and positive peaks occur during the isovolumic relaxation (3) and ventricular filling (4) phases, respectively.

Unlike acceleration for the viscous case, the peaks of acceleration for the elastic component do not match experimental findings, which suggests that the forces due to elastic deformations are relatively small. In the proceeding analysis, only acceleration for the viscous component is examined and discussed.

### Longitudinal displacement velocity

Since the sternum is located near the apex, SCG morphology is mostly affected by ventricular contraction in the longitudinal direction of the ventricles, which is reflected in the longitudinal displacement of the LV apex. The displacement velocity of the LV apex in the longitudinal direction is shown in Figure 1E. Indeed, the rapid increase of longitudinal velocity during the isovolumic phase (1) results in a negative peak in the SCG since the pressure on the rib cylinder decreases. The negative velocity peak, which follows this positive peak, is much smaller. Nevertheless, the rising LV intracavitary pressure amplifies the force acting on the rib cylinder, which, in turn, results in a pronounced positive peak of the SCG signal at the end of isovolumic contraction. The longitudinal displacement of the LV apex is further illustrated by the images of the anterior ventricular surface in Figure 1F. Indeed, at the end of isovolumic contraction, the longitudinal dimension of the ventricles decreases.

The peaks during the other phases of the cardiac cycle can be explained in a similar manner.

### Effect of rib orientation on SCG signal

Changes in orientation of the rib result in different peak amplitudes in SCG as well as different morphologies (Figure 1C). An additional positive peak appears at the beginning of isovolumic contraction and the amplitude of the negative peak is decreased. The magnitude of the SCG signal is different during ejection and isovolumic relaxation in the rotated case as compared to the control case. Lastly, there is a local positive peak during ventricular filling in the rotated case that is absent in the control case. These findings suggest that the changes in SCG morphology can be attributed to the different orientation of the rib with respect to the ventricles.

## **DISCUSSION**

This study employs a novel image-based anatomically-accurate model of ventricular contraction to provide insight into the SCG morphology. The main findings of this study are 1) the acceleration of the chest is due to the pressure of the heart acting on the chest and is mostly determined by the viscosity of the chest, 2) the isovolumic peaks of the SCG signal arise from the longitudinal contraction of the ventricles, 3) changes in SCG morphology during respiration are explained by variations in the orientation of the ribs relative to the heart.

### Changes in longitudinal displacement velocity underlie SCG morphology during isovolumic contraction

The negative and positive peaks during the isovolumic phase of contraction are key systolic features of SCG morphology. Our results demonstrate that the negative peak arises due to a decrease in the longitudinal dimension of the ventricles. During isovolumic contraction, the LV apex moves rapidly towards the base as noted by the increase in longitudinal velocity. Then, the longitudinal velocity is reduced at the end of isovolumic contraction. These changes in longitudinal velocity are consistent with experimental recordings of longitudinal strain [10], which show an initial rapid decrease with a subsequent brief slowing.

In the framework of our model, contraction in longitudinal direction is explained by the ventricular activation sequence and the fiber geometry of the heart. The electrical impulse travels through the Purkinje network to the endocardium, the inner most layer of the working myocardium. The endocardial myofibers are oriented mostly longitudinally due to the trabeculation. Activation of this myofibers results in the development of active stress in the longitudinal direction, which in turn leads to longitudinal contraction of the ventricles. Then, electrical activation propagates transmurally from endocardium to epicardium (outer layer of the ventricles), resulting in activation of myofibers oriented more circumferentially. As these layers contract, the short-axis diameter of the ventricles decreases, and since the ventricular volume is constant, the shortening of these circumferentially oriented myofibers impedes longitudinal contraction, leading to a positive peak in the SCG signal. Other factors that may determine the positive isovolumic peak in SCG signal include the asymmetry in contraction between the right and left ventricles and the increasing intracavitary pressure.

### Changes in rib orientation alter SCG morphology

Our current results demonstrate that changes in amplitude and morphology of the SCG signal can be due to the orientation of the heart relative to the chest during respiration. When the cylinder that represents the rib is oriented more in the longitudinal direction, there is an additional pressure on the rib from the right ventricular wall.

However, other possible mechanisms may also be considered. Specifically, the increased pulmonic pressure during inspiration elevates the afterload of the right ventricle and end-systolic right ventricular pressure [11], thus increasing the pressure of the ventricles acting on the chest. In addition, respiration

leads to changes in LV contraction. These alternative mechanisms will be tested in the future with our model.

## ACKNOWLEDGEMENTS

This study was supported by US NIH grants R01-HL063195, R01-HL082729 and R01-HL067322, and NSF grant CBET-0601935.

## REFERENCES

- [1] R. Crow, P. Hannan, D. Jacobs, L. Hedquist, and D. Salerno, "Relationship between seismocardiogram and echocardiogram for events in the cardiac cycle," *American journal of noninvasive cardiology*, vol. 8, pp. 39-46, 1994.
- [2] L. Giorgis, A. Hernandez, A. Amblard, L. Senhadji, S. Cazeau, E. Donal, and G. Jauvert, "Analysis of Cardiac Micro-Acceleration Signals for the Estimation of Systolic and Diastolic Time Intervals in Cardiac Resynchronization Therapy," in *35th International Conference on Computers in Cardiology*, Bologna, Italy, 2008, pp. 393-396.
- [3] B. Ngai, K. Tavakolian, A. Akhbardeh, A. Blaber, B. Kaminska, and A. Noordergraaf, "Comparative analysis of seismocardiogram waves with the ultra-low frequency ballistocardiogram," *Conference proceedings: Annual International Conference of the IEEE Engineering in Medicine and Biology Society.*, vol. 1, pp. 2851-2854, 2009.
- [4] K. Tavakolian, A. Vaseghi, and B. Kaminska, "Improvement of ballistocardiogram processing by inclusion of respiration information," *Physiological measurement*, vol. 29, pp. 771-781, 2008.
- [5] I. Korzeniowska-Kubacka, B. Kusmierczyk-Droszcz, M. Bilinska, B. Dobraszkiwicz-Wasilewska, K. Mazurek, and J. Piotrowicz, "Seismocardiography – a non-invasive method for assessing systolic and diastolic left ventricular function in ischemic heart disease," *Folia Cardiol*, vol. 13, pp. 319-325, 2006.
- [6] J. R. Libonati, A. M. Colby, T. M. Caldwell, R. Kasparian, and H. L. Glassberg, "Systolic and diastolic cardiac function time intervals and exercise capacity in women," *Medicine and science in sports and exercise*, vol. 31, pp. 258-263, 1999.
- [7] A. Akhbardeh, K. Tavakolian, V. Gurev, T. Lee, W. New, B. Kaminska, and N. Trayanova, "Comparative analysis of three different modalities for characterization of the seismocardiogram," *Conference proceedings: Annual International Conference of the IEEE Engineering in Medicine and Biology Society.*, vol. 1, pp. 2899-2903, 2009.
- [8] R. C. P. Kerckhoffs, S. N. Healy, T. P. Usyk, and A. D. McCulloch, "Computational Methods for Cardiac Electromechanics," *Proceedings of the IEEE*, vol. 94, pp. 769-783, 2006.
- [9] INRIA, Asclepios Research Project: [https://gforge.inria.fr/frs/?group\\_id=726](https://gforge.inria.fr/frs/?group_id=726)
- [10] T. Edvardsen, B. Gerber, J. r. m. Garot, D. Bluemke, J. o. Lima, and O. Smiseth, "Quantitative assessment of intrinsic regional myocardial deformation by Doppler strain rate echocardiography in humans: validation against three-dimensional tagged magnetic resonance imaging," *Circulation*, vol. 106, pp. 50-56, 2002.
- [11] F. Jardin, G. Delorme, A. Hardy, B. Auvert, A. Beauchet, and J. P. Bourdarias, "Reevaluation of hemodynamic consequences of positive pressure ventilation: emphasis on cyclic right ventricular afterloading by mechanical lung inflation," *Anesthesiology*, vol. 72, pp. 966-970, 1990.

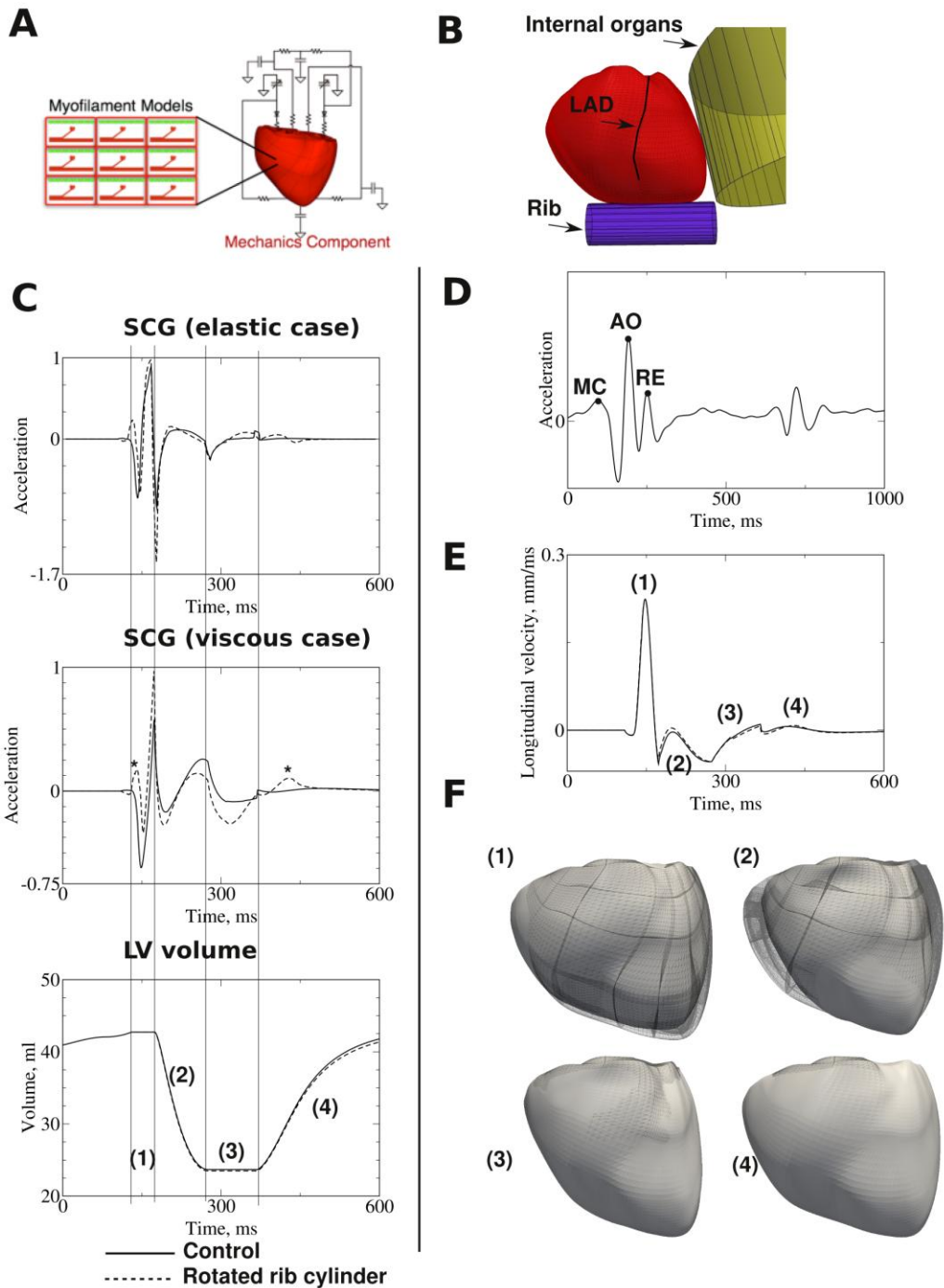


Figure 1: *Electromechanical model of ventricular contraction and simulation of SCG signal.* **A.** Diagram of electromechanical model coupled with the model of blood circulation in the body. **B.** Location of rib and thoracic organs in the model. **C.** Temporal traces of acceleration in the elastic case (top), acceleration in the viscous case (middle) and LV volume (bottom). Solid and dashed lines represent control and rotated rib orientation, respectively. Stars highlight changes in SCG morphology due to rotated rib. **D.** Clinically-recorded SCG signal. **E.** Longitudinal displacement velocity of LV apex. **F.** Deformations of the ventricles during different phases of cardiac cycle (view from the anterior surface). Notations: (1) – isovolumic contraction, (2) – ejection phase, (3) – isovolumic relaxation, (4) – ventricular filling, LAD – left anterior descending coronary artery. MC – mitral valve closing, AO – aortic valve opening, RE – rapid ejection.